Inorg. Chem. **2005**, *44*, 9763–9770

Between $Ni(mnt)_2$ and $Ni(tfd)_2$ Dithiolene Complexes: the Unsymmetrical 2-(Trifluoromethyl)acrylonitrile-1,2-dithiolate and Its Nickel Complexes

Olivier Jeannin,[†] Jacques Delaunay,[†] Frédéric Barrière,[‡] and Marc Fourmigué*[,†]

Laboratoire Chimie, Ingénierie Moléculaire et Matériaux (CIMMA), UMR 6200, CNRS, Université d'Angers, Bât K, UFR Sciences, 2 Bd Lavoisier, 49045 Angers, France, and Laboratoire d'Electrochimie Moléculaire et Macromoléculaire, SESO UMR 6510, Institut de Chimie de Rennes, Campus de Beaulieu, 35042 Rennes, France

Received July 22, 2005

A novel 1,2-dithiolate ligand, that is, the 2-(trifluoromethyl)acrylonitrile-1,2-dithiolate, abbreviated here as tfadt, is prepared from the corresponding cyclic dithiocarbonate. This ligand, substituted with both a CN and a CF_3 group, is compared with the well-known maleonitrile- and bis(trifluoromethyl)ethane-1,2-dithiolates. The preparation, electrochemical properties, and X-ray crystal structures of the square-planar nickel complexes, in both their dianionic diamagnetic $[Ni(tfadt)_2]^{2-}$ and their monoanionic paramagnetic $[Ni(tfadt)_2]^{\bullet-}$ forms, are reported, as n-Bu_4N^+, PPh_4^+, and (18-crown-6)Na^+ salts, respectively. In the $[(18\text{-crown-6})Na]_2[Ni(tfadt)_2]$ salt, each CN moiety of the $[Ni(tfadt)_2]^{2-}$ dianion is coordinated to a (18-crown-6)Na^+ cation through a CN···Na interaction [N···Na = 2.481(3) Å], affording an "axle with wheels" model where two MeOH molecules act as axle caps. On the other hand, in [(18-crown-6)-Na][$Ni(tfadt)_2$], each (18-crown-6)Na^+ cation is coordinated on both sides by the CN groups of two monoanionic $[Ni(tfadt)_2]^{\bullet-}$ complexes with N···Na^+ distances at 2.434(5) and 2.485(4) Å, giving rise to heterobimetallic chains with alternating (18-crown-6)Na^+ and $[Ni(tfadt)_2]^{\bullet-}$ ions. These two examples demonstrate the attractive ability of the CN moieties in the $[Ni(tfadt)_2]^{2-,\bullet-}$ complexes to coordinate metallic cationic centers. The paramagnetic salts of the anionic $[Ni(tfadt)_2]^{\bullet-}$ complex follow Curie-type law in the 2–300 K temperature range, indicating the absence of intermolecular magnetic interactions in the solid state. The complexes are found in their trans form in all crystal structures, while density functional theory calculations establish that both forms have essentially the same energy. A cis–trans interconversion process is observed by variable-temperature NMR on the dianionic $[Ni(tfadt)_2]^{2-}$ complex with a coalescence temperature T_c of 260 K and a free energy of activation of 51–53 kJ mol^{-1}.

Introduction

Coordination compounds of nitrile-containing radical anion species[1,2] such as those derived from tetracyanoethylene,[3] 7,7,8,8-tetracyanoquinodimethane,[4,5] tetrafluoro-7,7,8,8-tetracyanoquinodimethane,[6] or dicyanoquinone iodide[7,8] have found wide interest in material science as organic conductors and molecular magnets. The combination of the coordination ability of the nitrile groups, the readily accessible radical anion state, and the planarity of the molecules, allowing for extensive stacking and conduction band formation, has qualified these π-acceptor molecules as invaluable precursors of $S = {}^1/_2$ radical species for the elaboration of coordination networks incorporating not only d but also f[9,10] metallic elements. In that respect, it is all the most surprising that corresponding dithiolene complexes[11] such as, for example,

* To whom correspondence should be addressed. E-mail: marc.fourmigue@univ-angers.fr.
[†] CNRS, Université d'Angers.
[‡] Institut de Chimie de Rennes.

(1) Kaim, W.; Moscherosch, M. *Coord. Chem. Rev.* **1994**, *129*, 157.
(2) Martin, N.; Segura, J. L.; Seoane, C. *J. Mater. Chem.* **1997**, *7*, 1661.
(3) (a) Manriquez, J. M.; Yee, G. T.; McLean, R. S.; Epstein, A. J.; Miller, J. S. *Science* **1991**, *252*, 1415. (b) Miller, J. S.; Epstein, A. J. *Chem. Commun.* **1998**, 1319.
(4) (a) Hoffmann, S. K.; Corvan, P. J.; Singh, P.; Sethulekshmi, C. N.; Metzger, R. M.; Hatfield, W. E. *J. Am. Chem. Soc.* **1983**, *105*, 4608. (b) Schwartz, M.; Hatfield, W. E. *Inorg. Chem.* **1987**, *26*, 2823. (c) Heintz, R. A.; Zhao, H.; Ouyang, X.; Grandinetti, G.; Cowen, J.; Dunbar, K. R. *Inorg. Chem.* **1999**, *38*, 144 and references cited therein.
(5) (a) Vickers, E. B.; Giles, I. D.; Miller, J. S. *Chem. Mater.* **2005**, *17*, 1667. (b) Vickers, E. B.; Selby, T. D.; Thorum, M. S.; Taliaferro, M. L.; Miller, J. S. *Inorg. Chem.* **2004**, *43*, 6414.
(6) Hibbs, W.; Arif, A. M.; Botoshansky, M.; Kaftory, M.; Miller, J. S. *Inorg. Chem.* **2003**, *42*, 2311.
(7) (a) Hünig, S.; Herberth, E. *Chem. Rev.* **2004**, *104*, 5535. (b) Kato, R. *Bull. Chem. Soc. Jpn.* **2000**, *73*, 515.
(8) Sugiura, K.; Mikami, S.; Johnson, M. T.; Raebiger, J. W.; Miller, J. S.; Iwasaki, K.; Okada, Y.; Hino, S.; Sakata, Y. *J. Mater. Chem.* **2001**, *11*, 2152.

10.1021/ic051226b CCC: $30.25
Published on Web 12/02/2005

$Ni(mnt)_2^{\bullet-}$ (mnt: maleonitrile-1,2-dithiolate or 1,2-dicyanoethene-1,2-dithiolate), which exhibits the very same attractive features,[12,13] has not yet been engaged in coordination compounds with magnetic metallic cations. The very few reported examples of mnt complexes engaged in coordination compounds involving coordination through the CN moiety are limited indeed to dianionic complexes such as $Sn(mnt)_3^{2-}$ with a naked Na^+ cation,[14] $Cu(mnt)_2^{2-}$ and $Ni(mnt)_2^{2-}$ with $(18c6)Na^+$ (18c6: 18-crown-6),[15] or $Ni(mnt)_2^{2-}$ with a cationic 3,3′-(1,3-propanediyldinitrilo)bis(2-butanone oxime)-copper complex.[16] Note, however, that dithiooxalate (dto) complexes[17] such as the diamagnetic $Ni(dto)_2^{2-}$ or the paramagnetic $Cu(dto)_2^{2-}$ have already been engaged in ordered magnetic bimetallic chains incorporating d or f[18] metallic cations through coordination via the four sp_2 oxygen atoms of the complexes, demonstrating the pertinence of this approach.

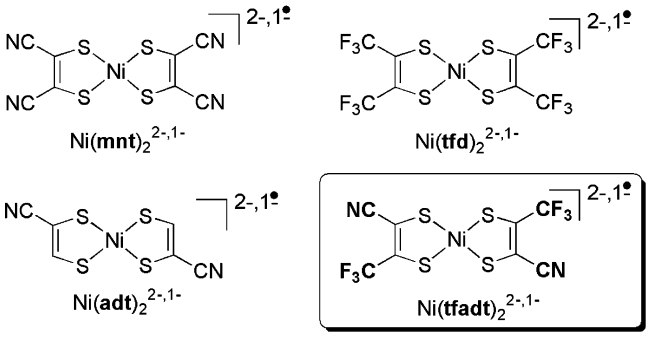

We recently reported that $Ni(mnt)_2^{\bullet-}$ and the analogous $Ni(adt)_2^{\bullet-}$ (adt: acrylonitrile-1,2-dithiolate) bearing only two CN groups[19] were indeed able to coordinate metallic centers such as the Mn^{III} complex of tetraphenylporphyrin (TPP),[20] affording unprecedented heterometallic ferrimagnetic chains involving dithiolene complexes, where the $S = 2$ cationic $Mn(TPP)^+$ and the $S = {}^1/_2$ anionic $Ni(mnt)_2^{\bullet-}$ or $Ni(adt)_2^{\bullet-}$ complexes alternate, with each Mn atom being axially coordinated by the nitrile of two different dithiolene complexes. We want here to extend the possibilities offered by the coordination of two CN groups in such dithiolene complexes and thus designed a novel dithiolate ligand, which associates both the CN group of the mnt or adt ligand and also the CF_3 group of the tfd ligand, that is, the 2-(trifluoromethyl)acrylonitrile-1,2-dithiolate, abbreviated here as tfadt. Indeed, by comparison with $Ni(mnt)_2^{2-,\bullet-}$ complexes, the presence of only two electron-withdrawing CN groups in the $Ni(adt)_2^{2-,\bullet-}$ complexes shifts the 2−/1− redox process to a more anodic potential,[19] an interesting feature because solutions of the anionic $Ni(mnt)_2^{\bullet-}$ exhibit a strong tendency to reduce to the diamagnetic $Ni(mnt)_2^{2-}$ dianion. On the other hand, with only one substituent on the dithiolate ligand, the $Ni(adt)_2^{\bullet-}$ complex is not very stable in solution and tends to decompose. It was therefore hoped that a dithiolate ligand incorporating still two substituents would be more chemically stable, while introduction of a CF_3 group, which is less electron-withdrawing than the CN group, would stabilize the radical anion $Ni(tfadt)_2^{\bullet-}$ complex by shifting the 2−/1− redox process toward more cathodic potentials when compared with $Ni(mnt)_2^{2-,\bullet-}$, as is indeed demonstrated here. We describe the synthesis of the 4-cyano-5-(trifluoromethyl)-1,3-dithiol-2-one precursor of the tfadt ligand, the preparation of the dianionic and monoanionic $Ni(tfadt)_2^{2-,\bullet-}$ complexes as n-Bu_4N^+ and Ph_4P^+ salts, and their X-ray crystal structures and magnetic properties. Furthermore, both dianionic and monoanionic complexes were isolated as Na^+ salts in the presence of 18c6, affording the first examples of metal coordination through the nitrile group with those complexes. The unsymmetrical character of the dithiolate ligand makes it possible for the first time to evaluate experimentally the inversion barrier for cis−trans isomerization, and ^{19}F variable-temperature (VT) NMR experiments were accordingly performed on the diamagnetic dianionic species and compared with the results of density functional theory (DFT) calculations.

Experimental Section

Syntheses. All reagents are commercially available unless otherwise stated. Dry solvents were obtained by distillation as indicated: tetrahydrofuran (THF) on Na/benzophenone, CH_2Cl_2 on P_2O_5, and MeOH on Mg. NMR spectra were recorded at 500.04 MHz for ^1H, 125.75 MHz for ^{13}C, and 470.282 MHz for ^{19}F. Mass spectrometry was performed in the electron ionization high-resolution mass spectrometry (EI−HRMS) mode for **2**−**4** and in the matrix-assisted laser desorption ionization time of flight (MALDI-ToF) mode for the **5a**, **5c**, **6a**, and **6c** salts.

4-(Trifluoromethyl)-5-amido-2-thioxo-1,3-dithiole (2). 4-(Trifluoromethyl)-5-(carbomethoxy)-2-thioxo-1,3-dithiole (**1**; 0.42 g, 1.61 mmol) is dissolved in dry THF (10 mL) and the solution cooled in a dry ice/acetone bath. Ammonia (10 mL) is then condensed into this solution, and the mixture is stirred for 45 min. Ammonia and solvent are evaporated at low temperature, and the crude product is dissolved in a minimum of acetonitrile. Layering with hexane afforded **2** as yellow needles (0.36 g, 1.47 mmol, 92%). Mp: 126.2 °C. ^1H NMR (acetone-d_6): δ 7.68 (d). ^{19}F NMR (acetone-d_6): δ −57.45 (s). Anal. Calcd for $C_5H_2F_3OS_3$: C, 24.48; H, 0.82; N, 5.71. Found: C, 24.46; H, 0.83; N, 5.71. HRMS *m*/*z*: calcd, 244.9251; found, 244.9271.

(9) Madalan, A. M.; Roesky, H. W.; Andruh, M.; Noltemeyer, M.; Stanica, N. *Chem. Commun.* **2002**, 1638.
(10) Raebiger, J. W.; Miller, J. S. *Inorg. Chem.* **2002**, *41*, 3308.
(11) Dithiolene Chemistry, Syntheses, Properties and Applications. In *Progress in Inorganic Chemistry*; Stiefel, E. I., Ed.; Wiley: New York, 2004; Vol. 52.
(12) Clemenson, P. I. *Coord. Chem. Rev.* **1990**, *106*, 171.
(13) Robertson, N.; Cronin, L. *Coord. Chem. Rev.* **2002**, *227*, 93.
(14) Day, R. O.; Holmes, J. M.; Shafieezad, S.; Chandrasekhar, V.; Holmes, R. R. *J. Am. Chem. Soc.* **1988**, *110*, 5377.
(15) Dou, J.-M.; Li, D.-C.; Yu, Q.-J.; Liu, Y.; Xu, L.-Q.; Bi, W. H.; Yong, W.; Zheng, P.-J. *Huaxue Xuebao* **2001**, *59*, 2162 (CCDC codes: XOQVUU and XOQWAB).
(16) Ren, X.; Duan, C.; Zhu, H.; Meng, Q.; Hu, C.; Lu, C.; Liu, Y. *Transition Met. Chem. (N.Y.)* **2001**, *26*, 295 (CCDC code: QEVJAZ).
(17) (a) Gleizes, A.; Verdaguer, M. *J. Am. Chem. Soc.* **1984**, *106*, 3727. (b) Gleizes, A.; Verdaguer, M. *J. Am. Chem. Soc.* **1981**, *103*, 7373.
(18) (a) Trombe, J. C.; Gleizes, A.; Dahan, F.; Galy, J. *C. R. Acad. Sci. Paris, Sér. II* **1986**, *302*, 21 and 907 and references cited therein. (b) Siebold, M.; Strauch, P. In *Advances in the Coordination of Bioinorganic and Inorganic Chemistry*; Melnick, M., Sima, J., Tatarko, M., Eds.; Slovak Technical University Press: Bratislava, Slovakia, 2005.
(19) Fourmigué, M.; Bertran, J. N. *Chem. Commun.* **2000**, 2111.
(20) Dawe, L. N.; Miglioi, J.; Turnbow, L.; Taliaferro, M. L.; Shum, W. W.; Bagnato, J. D.; Zakharov, L. N.; Rheingold, A. L.; Arif, A. M.; Fourmigué, M.; Miller, J. S. *Inorg. Chem.* **2005**, *44*, 7530.

4-(Trifluoromethyl)-5-cyano-2-thioxo-1,3-dithiole (3). 2 (0.15 g, 0.61 mmol) is dissolved in sulfolane (2.5 mL), $POCl_3$ (0.15 mL, 1.6 mmol) is added, and the mixture is heated for 4 h at 100 °C. The dark solution is poured in ice/water (50 mL) and extracted twice with pentane (2 × 75 mL). After drying over $MgSO_4$ and evaporation of the solvent, the residual oil is purified by chromatography on silica gel (eluant: 3:1 pentane/CH_2Cl_2), affording **3** as an orange oil (89 mg, 0.39 mmol, 64%). ^{19}F NMR ($CDCl_3$): δ −58.61 (s). ^{13}C NMR ($CDCl_3$): 106.21 (s), 113.34 (q, $^3J_{C-F}$ = 3.37 Hz.), 117.33 (q, $^1J_{C-F}$ = 274.37 Hz), 142.52 (q, $^2J_{C-F}$ = 38.37 Hz.), 201.11 (s). Anal. Calcd for $C_5F_3NS_3$: C, 26.43; N, 6.16. Found: C, 26.58; N, 6.87. HRMS *m*/*z*: calcd, 226.9145; found, 226.9148.

4-(Trifluoromethyl)-5-cyano-2-oxo-1,3-dithiole (4). 3 (5.26 g, 0.023 mol) is dissolved in a CH_2Cl_2/acetic acid mixture (3:1, 400 mL). Mercuric acetate (16.23 g, 0.051 mol) is added at once. The suspension is stirred for 2.5 h and filtered on Celite. The organic part is washed with saturated Na_2CO_3 and water and dried with $MgSO_4$ to give a yellow oil. Chromatography on silica gel with CH_2Cl_2 gives **4** as a pale-yellow oil (4.29 g, 0.02 mol, 88%). ^{19}F NMR ($CDCl_3$): δ −57.76 (s). ^{13}C NMR ($CDCl_3$): 105.79 (q, $^3J_{C-F}$ = 3.5 Hz.) 107.46 (s), 118.48 (q, $^1J_{C-F}$ = 273.75 Hz), 135.54 (q, $^2J_{C-F}$ = 38.25 Hz.), 198.07 (s). Anal. Calcd for $C_5F_3NOS_2$: C, 28.44; N, 6.63. Found: C, 27.09; N, 7.71.

(*n*-Bu$_4$N)$_2$[Ni(tfadt)$_2$] (5a). Under nitrogen, **4** (0.25 g, 1.18 mmol) is added to a solution of sodium (0.06 g, 2.6 mmol) in dry MeOH (5 mL) to give a pale-green solution. After stirring for 45 min, $NiCl_2(H_2O)_6$ (0.14 g, 0.59 mmol) is added, giving a dark-red solution. The addition of (*n*-Bu$_4$N)Br (0.38 g, 1.18 mmol) followed by water (70 mL) afforded an orange-red precipitate. After filtration, washings with water, and drying, the product is recrystallized in an ethanol/water mixture to give **5a** as orange-red needles suitable for X-ray analysis (0.42 g, 0.46 mmol, 77.7%). Mp: 156 °C. ν (KBr): 2201.96 (CN) cm^{-1}. ^{19}F NMR (CD_2Cl_2): δ −58.68 (s). Anal. Calcd for $C_{40}H_{72}F_6N_4NiS_4$: C, 52.79; H, 7.97; N, 6.16. Found: C, 52.69; H, 8.11 N, 6.07. MALDI-TOF (negative mode): found, 423.76 corresponding to [Ni(tfadt)$_2$]$^-$; calcd, 423.82.

(*n*-Bu$_4$N)[Ni(tfadt)$_2$] (6a). Ferricinium tetrafluoroborate (0.07 g, 0.25 mmol) is dissolved in dry CH_2Cl_2 (4 mL) under nitrogen, and **5a** (0.23 g, 0.25 mmol) is then added to the blue solution. After stirring for 1 h, pentane (70 mL) is added to the black solution. The yellow pentane phase and the black oil are separated. Dissolution of the black oil in CH_2Cl_2 and layering with pentane give low-quality crystals of **6a**. A second layering with pentane gives suitable black crystals of **6a** (0.1 g, 0.15 mmol, 60%). Mp: 120 °C. ν (KBr): 2214.17 (CN) cm^{-1}. Anal. Calcd for $C_{24}H_{36}F_6N_3NiS_4$: C, 43.18; H, 5.44; N, 6.29. Found: C, 43.05; H, 5.39; N, 6.02. MALDI-TOF (negative mode): found, 423.80 corresponding to [Ni(tfadt)$_2$]$^-$; calcd, 423.82.

(PPh$_4$)$_2$[Ni(tfadt)$_2$] (5b). This compound is prepared according to the procedure applied for synthesis of the corresponding **5a** salt using PPh_4Br in the metathesis reaction. Recrystallization is carried out in acetone with Et_2O layering to give **5b** as orange thin plates (60%). Mp: 271 °C. Anal. Calcd for $C_{56}H_{40}F_6N_2NiP_2S_4$: C, 60.93; H, 3.65; N, 2.54. Found: C, 61.01; H, 3.88; N, 2.27.

(PPh$_4$)[Ni(tfadt)$_2$] (6b). Under nitrogen, ferricinium tetrafluoroborate (0.08 g, 0.29 mmol) is added to a suspension of **5b** (0.32 g, 0.3 mmol) in dry CH_2Cl_2 (20 mL). Dissolution of the dianion rapidly occurs, giving a black solution. The product is precipitated by the addition of pentane, filtered, and washed with pentane and Et_2O. Washing with acetone yields a pale-yellow residue. Evaporation of the acetone filtrate followed by washing with a 1:1 Et_2O/ethyl acetate mixture yields a brown powder after removal of the solvents. Layering of a CH_2Cl_2 solution with pentane gives **6b** as brown needles (0.13 g, 0.17 mmol, 59%). Mp: 216 °C. Anal. Calcd for $C_{32}H_{20}F_6N_2NiPS_4$: C, 50.28; H, 2.64; N, 3.66. Found: C, 50.05; H, 2.55; N, 3.44.

[Na(18c6)]$_2$[Ni(tfadt)$_2$] (5c). 4 (0.3 g, 1.32 mmol) is added to a solution of sodium (0.068 g, 2.9 mmol) in dry MeOH (5 mL) to give a pale-green solution. After stirring for 45 min, $NiCl_2(H_2O)_6$ (0.15 g 0.63 mmol) is added, giving a dark-red solution, which is stirred for 2 h. The mixture is filtered on Celite and poured into a solution of 18c6 (0.4 g, 1.5 mmol) in MeOH (1 mL). Layering with pentane gives orange crystals. Dissolution of these crystals in MeOH followed by filtration and layering with pentane give orange crystals of formulation [Na(18c6)]$_2$[Ni(tfadt)$_2$][MeOH]$_2$, that is, **5c**·2MeOH, based on the X-ray crystal structure determination (see below). Drying these crystals for 2 weeks (vacuum, P_2O_5) afforded the unsolvated complex **5c** (0.43 g, 0.43 mmol, 68%) as an orange powder. Mp: 236 °C. ν (KBr): 2209.03 (CN) cm^{-1}. Anal. Calcd for **5c**: $C_{32}H_{48}F_6N_2Na_2NiO_{12}S_4$: C, 38.45; H, 4.84; N, 2.8. Found: C, 37.68; H, 4.73; N, 2.42. MALDI-TOF (negative mode): found, 423.86 corresponding to [Ni(tfadt)$_2$]$^-$; calcd, 423.82. MALDI-TOF (positive mode): found, 287.11 corresponding to [(18c6)Na]$^+$; calcd, 287.15.

[Na(18c6)][Ni(tfadt)$_2$] (6c). 5c (0.3 g, 0.3 mmol) is dissolved in dimethyl sulfoxide (DMSO; 3 mL), and iodine (0.099 g, 0.39 mmol) in DMSO (2 mL) is added to the red solution. The solution turns black, it is stirred for 2.5 h, and the product precipitated by the addition of water (90 mL). The filtered black powder is washed with water and dried by coevaporation with absolute ethanol. The dried black powder is purified by layering pentane on a CH_2Cl_2 solution to give **6c** as black needles (0.15 g, 0.21 mmol, 70%) suitable for X-ray crystal structure determination. Mp: 135 °C (dec), 169 °C (melting). ν (KBr): 2217.19 (CN) cm^{-1}. Anal. Calcd for $C_{20}H_{24}F_6N_2NaNiO_6S_4$: C, 33.72; H, 3.39; N, 3.93. Found: C, 33.39; H, 3.21; N, 3.65. MALDI-TOF (negative mode): found, 424.28 corresponding to [Ni(tfadt)$_2$]$^-$; calcd, 423.82. MALDI-TOF (positive mode): found, 287.20 corresponding to [(18c6)Na]$^+$; calcd, 287.15.

Crystallographic Data Collection and Structure Determination. Crystals were mounted on top of a thin glass fiber. Crystals of **5c**·2MeOH rapidly lose the MeOH solvent molecules at room temperature. They were transferred in mineral oil, glued on a thin glass capillary, and cooled rapidly to 150 K at 120 K/min for the data collection. Data were collected on a Stoe Imaging Plate Diffraction System (IPDS) with graphite-monochromatized Mo Kα radiation (λ = 0.710 73 Å). The crystal data are summarized in Table 1. Structures were solved by direct methods (SHELXS-97) and refined by full matrix least-squares methods (SHELXL-97). Absorption corrections were applied for all structures. Hydrogen atoms were introduced at calculated positions (riding model), included in structure factor calculations, and not refined.

Magnetic Measurements. Magnetic susceptibility measurements were performed on a Quantum Design MPMS-2 SQUID magnetometer operating in the range 2−300 K at 5000 G with polycrystalline samples of **6a**−**c**. Gelatin capsules were used with a magnetization contribution of $-2.37 \times 10^{-6} + [2.2 \times 10^{-6}/(T + 2)]$ emu G g^{-1}, which was used for correction of the experimental magnetization. Molar susceptibilities were then corrected for Pascal diamagnetism.

Computational Details. DFT[21] calculations were performed with the hybrid Becke-3 parameter exchange functional[22] and the Lee−Yang−Parr nonlocal correlation functional[23] (B3LYP) implemented in the *Gaussian 03* (revision B.05) program suite[24] using the LANL2DZ basis set[25] and a quadratically convergent self-consistent-field procedure[26] with the default convergence criteria implemented

Table 1. Crystallographic Data

compound	**5a**	**5b**	**5c**·2MeOH	**6a**	**6b**	**6c**
formula	$C_{40}H_{72}F_6N_4NiS_4$	$C_{56}H_{40}F_6N_2NiP_2S_4$	$C_{34}H_{54}F_6N_2Na_2NiO_{14}S_4$	$C_{24}H_{36}F_6N_3NiS_4$	$C_{32}H_{20}F_6N_2NiPS_4$	$C_{20}H_{24}F_6N_2NaNiO_6S_4$
fw	909.97	1103.79	1061.72	667.51	764.42	712.37
cryst syst	monoclinic	monoclinic	monoclinic	monoclinic	monoclinic	monoclinic
space group	$P2_1/n$	$P2_1/n$	$C2/c$	$C2/c$	$C2/c$	$P2_1/c$
a/Å	15.1833(11)	13.9167(16)	28.350(6)	25.175(5)	25.585(2)	7.9125(16)
b/Å	21.8800(14)	13.8219(11)	10.787(2)	8.6412(17)	8.2118(4)	15.458(3)
c/Å	15.5033(10)	14.4331(15)	17.958(4)	16.091(3)	17.6127(14)	24.159(5)
α/deg	90.0	90.0	90.0	90.	90.0	90.0
β/deg	112.440(7)	110.824(12)	119.99(3)	117.04(3)	116.730(8)	92.78(3)
γ/deg	90.0	90.0	90.0	90.	90.0	90.0
V/Å^3	4760.4(6)	2594.9(5)	4756.4(17)	3117.8(11)	3305.0(4)	2951.4(10)
Z	4	2	4	4	4	4
d_{calc}/Mg m^{-3}	1.270	1.413	1.483	1.422	1.536	1.603
diffraction	Stoe IPDS	Stoe IPDS	Stoe IPDS	Stoe IPDS	Stoe IPDS	Stoe IPDS
temp/K	150(2)	293	150(2)	150(2)	293(2)	293(2)
μ/mm^{-1}	0.638	0.658	0.686	0.945	0.948	1.03
θ range/deg	1.85−25.82	2.11−25.77	2.06, 25.79	2.53, 25.78	1.78−25.81	2.14, 26.00
meas reflns	36395	19425	22537	14649	15506	22133
indep reflns	9108	4920	4328	2876	3148	5719
R_{int}	0.081	0.116	0.088	0.052	0.0351	0.109
I > 2σ(I) reflns	5692	2042	2779	2261	2230	2643
abs corr	multiscan	multiscan	multiscan	multiscan	multiscan	Gaussian
T_{max}, T_{min}	0.869, 0.809	0.874, 0.788	0.913, 0.856	0.769, 0.686	0.823, 0.706	0.961, 0.724
refined param	496	322	314	228	237	382
R(F), $I > 2\sigma(I)$	0.0373	0.0522	0.0362	0.0441	0.0312	0.0423
wR(F^2), all	0.0834	0.1351	0.0822	0.1308	0.0828	0.0853
$\Delta\rho$ (e Å^{-3})	+0.51, −0.46	+0.69, −0.35	+0.39, −0.46	+1.05, −0.37	+0.22, −0.27	+0.25, −0.23

in the program. Every stationary point calculation was subjected to analytical vibrational frequency analysis, which confirmed its optimized stationary point nature, with all frequencies being positive. The tetrahedral intermediate was built from the optimized trans-planar structures and then subjected to a single-point calculation to get an estimate of the cis−trans interconversion energy barrier. Frequency calculation on these models showed that they were not true saddle points, with more than one frequency being negative, introducing a slight error in the estimation of the interconversion energy barrier.

Results and Discussion

Syntheses. The dithiocarbonate **4** necessary for the formation of the complexes has been obtained (Scheme 1) from the corresponding ester derivative **1** by adapting a procedure described for 4-cyano-1,3-dithiole-2-one, the precursor of the adt ligand. Reaction of the trithiocarbonate **1** with dry NH_3 in THF at −78 °C afforded the primary amide **2**, which was then dehydrated with $POCl_3$ to the nitrile **3** and treated with $Hg(OAc)_2$ to afford **4** as a pale-yellow oil.

Scheme 1

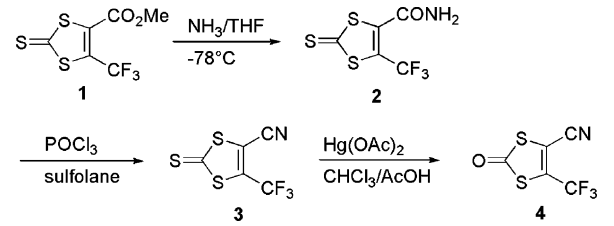

Scheme 2

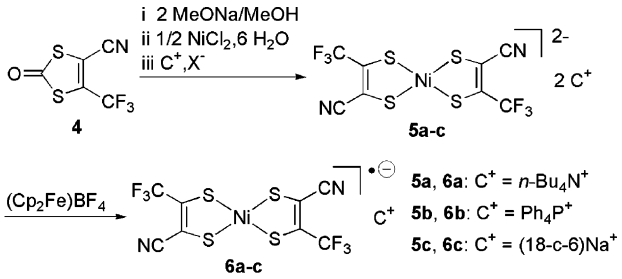

The dianionic complexes $Ni(tfadt)_2^{2-}$ were prepared (Scheme 2) from the dithiocarbonate **4** by treatment with sodium methanolate, addition of $NiCl_2 \cdot 6H_2O$, and precipitation of the intermediate sodium salt with either n-Bu_4NBr, PPh_4Br, or 18c6 to afford **5a**, **5b**, and **5c**, respectively, as red crystalline material. Oxidation of the dianionic complexes **5a**−**c** with iodine afforded the corresponding oxidized radical anion species **6a**−**c** but in an impure form because of the difficulty of removing residual n-Bu_4NI_3. Alternatively, the

(21) (a) Hohenberg, P.; Kohn, W. *Phys. Rev.* **1964**, *136*, B864. (b) Parr, R. G.; Yang, W. *Density-Functional Theory of Atoms and Molecules*; Oxford University Press: Oxford, U.K., 1989.
(22) (a) Becke, A. D. *Phys. Rev. A* **1988**, *38*, 3098. (b) Becke, A. D. *J. Chem. Phys.* **1993**, *98*, 1372. (c) Becke, A. D. *J. Chem. Phys.* **1993**, *98*, 5648.
(23) Lee, C.; Yang, W.; Parr, R. G. *Phys. Rev. B* **1988**, *37*, 785.
(24) Frisch, M. J.; Trucks, G. W.; Schlegel, H. B.; Scuseria, G. E.; Robb, M. A.; Cheeseman, J. R.; Montgomery, J. A., Jr.; Kudin, K. N.; Burant, J. C.; Millam, J. M.; Iyengar, S. S.; Tomasi, J.; Barone, V.; Mennucci, B.; Cossi, M.; Scalmani, G.; Rega, N.; Petersson, G. A.; Nakatsuji, H.; Hada, M.; Ehara, M.; Toyota, K.; Fukuda, R.; Hasegawa, J.; Ishida, M.; Nakajima, T.; Honda, Y.; Kitao, O.; Nakai, H.; Klene, M.; Li, X.; Knox, J. E.; Hratchian, H. P.; Cross, J. B.; Adamo, C.; Jaramillo, J.; Gomperts, R.; Stratmann, R. E.; Yazyev, O.; Austin, A. J.; Cammi, R.; Pomelli, C.; Ochterski, J. W.; Ayala, P. Y.; Morokuma, K.; Voth, G. A.; Salvador, P.; Dannenberg, J. J.; Zakrzewski, G.; Dapprich, S.; Daniels, A. D.; Strain, M. C.; Farkas, O.; Malick, D. K.; Rabuck, A. D.; Raghavachari, K.; Foresman, J. B.; Ortiz, J. V.; Cui, Q.; Baboul, A. G.; Clifford, S.; Cioslowski, J.; Stefanov, B. B.; Liu, G.; Liashenko, A.; Piskorz, P.; Komaromi, I.; Martin, R. L.; Fox, D. J.; Keith, T.; Al-Laham, M. A.; Peng, C. Y.; Nanayakkara, A.; Challacombe, M.; Gill, P. M. W.; Johnson, B.; Chen, W.; Wong, M. W.; Gonzalez, C.; Pople, J. A. *Gaussian 03*, revision B.05; Gaussian, Inc.: Pittsburgh, PA, 2003.
(25) (a) Wadt, W. R.; Hay, P. J. *J. Chem. Phys.* **1985**, *82*, 284. (b) Hay, P. J.; Wadt, W. R. *J. Chem. Phys.* **1985**, *82*, 299.
(26) Bacskay, G. B. *Chem. Phys.* **1981**, *61*, 385.

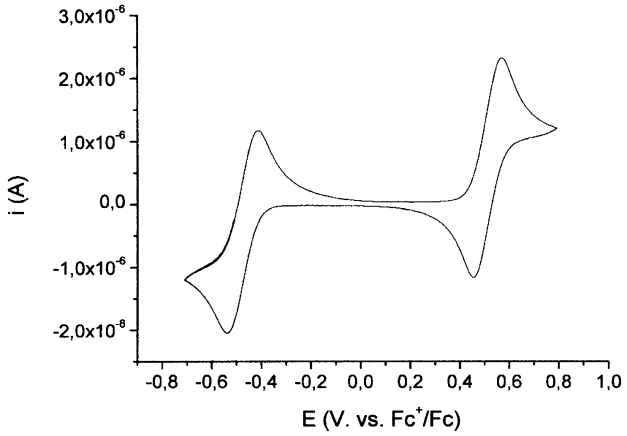

Figure 1. Cyclic voltammogram of **5a** (10^{-2} M in CH_2Cl_2, 0.05 M *n*-Bu_4NPF_6, $\nu = 100$ mV s^{-1}).

Table 2. Cyclic Voltammetry Data[a]

compound	$E_{1/2}^{-2/-}$	$E_{1/2}^{-/0}$	ref
(*n*-$Bu_4N)_2$[Ni(mnt)$_2$]	−0.16 (0.24)	+0.63 (+1.03)	28
(*n*-$Bu_4N)_2$[Ni(tfadt)$_2$][b]	−0.45	+0.51	this work
[Na(18c6)]$_2$[Ni(tfadt)$_2$][c]	−0.46	+0.51	this work
[Na(18c6)]$_2$Ni(tfadt)$_2$] in [Na(18c6)]PF_6[d]	−0.55	+0.50	this work
(*n*-$Bu_4N)_2$[Ni(tfd)$_2$]	−0.51 (−0.11)	+0.53 (+0.93)	28
(*n*-$Bu_4N)_2$[Ni(adt)$_2$]	−0.70 (−0.30)	+0.26 (+0.66)	19

[a] *E* in V vs Fc^+/Fc. Values reported vs SCE for the mnt, tfd, and adt complexes are given in parentheses and have been corrected by −0.40 V for comparison purposes.[27] [b] 10^{-2} M Ni(tfadt)$_2$ in CH_2Cl_2/0.05 M *n*-Bu_4NPF_6. [c] 10^{-3} M [Na(18c6)$_2$][Ni(tfadt)$_2$] in CH_2Cl_2/0.05 M *n*-Bu_4NPF_6. [d] 10^{-3} M [Na(18c6)$_2$][Ni(tfadt)$_2$] in CH_2Cl_2/0.05 M Na(18c6).

oxidation was conducted with ferricinium tetrafluoroborate and afforded **6a**−**c** in pure form.

Electrochemical Properties. Electrochemical characterizations were investigated by cyclic voltammetry on the dianionic **5a** species in CH_2Cl_2 with 0.05 M *n*-Bu_4NPF_6 as the electrolyte. The complexes exhibit two reversible redox waves, attributed to the 2−/1− and 1−/0 redox processes (Figure 1 and Table 2).

Values of the $E^{1/2}$ potentials are, as expected, between those reported for the symmetrical mnt and tfd complexes,[28] i.e., Ni(mnt)$_2^{2-,-,0}$ and Ni(tfd)$_2^{2-,-,0}$. Note, however, that the redox potentials of the Ni(tfadt)$_2$ system are close to those reported for the Ni(tfd)$_2$ system, indicating some kind of cooperativity in the electron-withdrawing effect of the two nitrile substituents in the mnt complexes. Similarly, the introduction of one CF_3 group on the adt ligand shifts the redox potentials toward cathodic potentials as expected. Of particular note is the reversible redox behavior for the 1−/0 process. Indeed, while the neutral Ni(tfd)$_2^0$ species is well-known and has been isolated in the solid state, the oxidation of Ni(mnt)$_2^-$ or Ni(adt)$_2^-$ to the neutral species had been reported to be irreversible until Geiger et al. demonstrated that reversibility of the Ni(mnt)$_2^{-/0}$ process could be recovered in dilute CH_2Cl_2 solutions of 10^{-3} M or less.[29] We

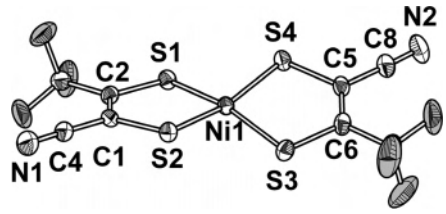

Figure 2. ORTEP view of [Ni(tfadt)$_2$]$^{2-}$ in **5a** (at 150 K) with thermal ellipsoids at the 50% probability level. Fluorine atoms have been darkened.

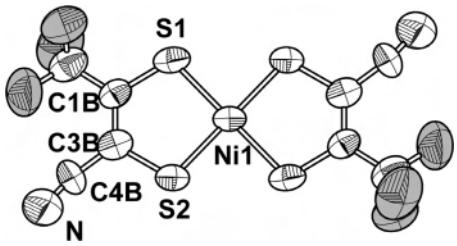

Figure 3. ORTEP view of [Ni(tfadt)$_2$]$^{2-}$ in **5b** (at 293 K) with thermal ellipsoids at the 50% probability level. Fluorine atoms have been darkened.

observed that, for concentrations up to 10^{-2} M, the reversibility of the 1−/0 process in Ni(tfadt)$_2^{\bullet -/0}$ was preserved, demonstrating that, in this respect, the tfadt ligand lies closer to tfd than to mnt. To test the ability of the nitrile group in [Ni(tfadt)$_2$]$^{2-,-,0}$ to coordinate cationic metal centers, a preliminary electrochemical experiment was performed with a 0.05 M solution of Na(18c6)PF_6 as the electrolyte, instead of the usual 0.05 M *n*-Bu_4NPF_6 conditions (Table 2). While the 1−/0 redox process is essentially unaffected by the electrolyte substitution, the 2−/1− redox process is shifted toward cathodic potentials by 90 mV, a clear indication of coordination of the nitrile substituents by the cationic Na(18c6)$^+$ moiety under those conditions where the cationic species is in a 50-fold excess relative to the electroactive complex.

Molecular and Solid-State Structures. The salts of the dianionic complexes, **5a** and **5b**, crystallize in the monoclinic system, space group $P2_1/n$, while **5c**·2MeOH crystallizes in the space group $C2/c$. The complex is located in a general position in **5a** (Figure 2) and on an inversion center in **5b** (Figure 3) and **5c**·2MeOH, while in the three cases, a trans conformation is observed. Of particular note is the large deviation from a perfect square-planar geometry around the Ni atom in the *n*-Bu_4N^+ salt **5a** (Figure 2) because the dihedral angle between the Ni−S1−S2 and Ni−S3−S4 mean planes amounts here to 21.91(5)°, while no deviation is observed in the two other salts, where the nickel atom is located on the inversion center. On the other hand, in the three salts of the monoanionic [Ni(tfadt)$_2$]$^{\bullet -}$ species, the complex is located on inversion centers and accordingly in a perfect square-planar environment.

Important bond lengths within the NiS_2C_2 metallacycle have been collected in Table 3. When going from the dianionic to the monoanionic complexes, we observed the recurrent shortening of the Ni−S (a and a′) and S−C (b and b′) single bonds with the concomitant lengthening of the C═C (c) double bond, a consequence of the antibonding character of the former and the bonding character of the latter, in the highest occupied molecular orbital (HOMO) of

(27) Connelly, N. G.; Geiger, W. E. *Chem. Rev.* **1996**, *96*, 877.
(28) Geiger, W. E.; Mines, T. E.; Senfleber, F. C. *Inorg. Chem.* **1975**, *14*, 2142.
(29) Geiger, W. E.; Barrière, F.; LeSuer, R. J.; Trupia, S. *Inorg. Chem.* **2001**, *40*, 2472.

Table 3. Important Bond Lengths (in Å) within the Metallacycles in **5a**−**c** and **6a**−**c**

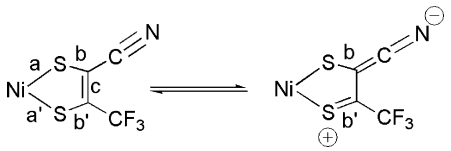

compd	bond length (Å) a	a′	b	b′	c	δ (%)[a]
			$[Ni(tfadt)]_2^{2-}$			
5a	2.1634(7)	2.1697(7)	1.748(3)	1.731(3)	1.365(4)	0.97
	2.1698(8)	2.1657(7)	1.745(3)	1.723(3)	1.356(4)	0.57
5b	2.162(1)	2.173(1)	1.740(6)	1.735(6)	1.346(7)	0.28
5c	2.1723(8)	2.1724(8)	1.749(3)	1.726(3)	1.359(3)	1.31
ave	2.167	2.170	1.745	1.729	1.356	0.92
	2.299	2.301	1.816	1.804	1.381	0.66
			$[Ni(tfadt)_2]^{\bullet-}$			
6a	2.1318(9)	2.1406(9)	1.729(3)	1.707(3)	1.355(5)	1.27
6b	2.1459(6)	2.1371(6)	1.726(3)	1.709(2)	1.355(3)	0.98
6c	2.141(1)	2.148(1)	1.721(4)	1.699(4)	1.361(6)	1.28
	2.139(1)	2.135(1)	1.727(4)	1.701(4)	1.361(6)	1.50
ave	2.139	2.140	1.726	1.704	1.358	1.30
	2.258	2.259	1.799	1.785	1.381	0.78

[a] $\delta = 100(b - b')/b$. DFT-calculated values are in italics (see text).

dianionic nickel dithiolene complexes. Another feature appears from Table 3 that is specific of this unsymmetrical dithiolate tfadt ligand, that is, a S−C bond length difference within the metallacycle, with a systematic shortening of the b′ bond when compared with the b bond, in the dianionic as well as in the monoanionic complexes. A similar effect has already been observed in the adt complex $Ni(adt)_2^{2-,\bullet-}$ and is attributed to the negative mesomeric effect of the nitrile substituent (see the scheme in Table 3). Contribution of the charge-separated mesomeric form thus leads to a shortening of the b′ C−S bond when compared with the b bond. This effect, evaluated as $\delta = 100(b - b')/b$, is observed between 0.28 and 1.50% in the six structures described here, while larger δ values were reported in $Ni(adt)_2^{2-}$ and $Ni(adt)_2^{\bullet-}$, 2.05 and 1.73%, respectively. This is most probably attributable to a compensating effect of the electron-withdrawing CF_3 group. DFT calculations performed on both dianionic (RB3LYP and LanL2DZ) and monoanionic (UB3LYP and LanL2DZ) complexes afforded optimized structures with intramolecular bond lengths slightly longer than those observed experimentally (Table 3). On the other hand, the trends described above are well represented, i.e., (i) the recurrent shortening of the Ni−S and C−S bond lengths upon oxidation from the dianion to the monoanion species, due to the antibonding character of those bonds in the dianion's HOMO and (ii) the differentiation between the b and b′ C−S bonds and its increase in the oxidized complex.

In the solid state, the dianionic $[Ni(tfadt)_2]^{2-}$ species are interspersed with *n*-Bu_4N^+ or PPh_4^+ cations and are thus completely isolated from each other (Figures S1 and S2 in the Supporting Information). In **6a**, the *n*-Bu_4N^+ salt of the monoanionic $Ni(tfadt)_2^{\bullet-}$, one nickel complex is located on an inversion center while the *n*-Bu_4N^+ cation lies on the 2-fold axis, giving rise to columns of $Ni(tfadt)_2^{\bullet-}$ running along *b* (Figure 4). However, the shortest intermolecular S···S distance exceeds 7.14 Å, preventing any possible

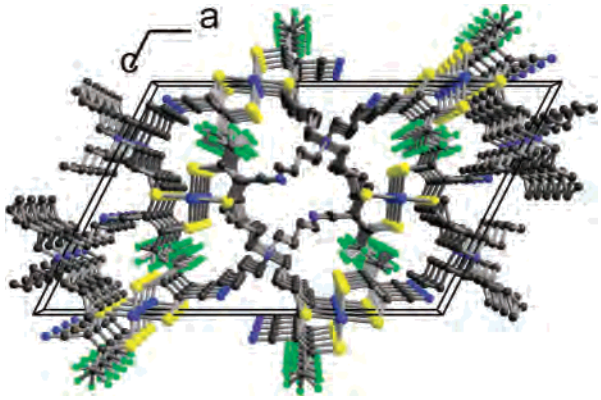

Figure 4. View of the salt **6a**.

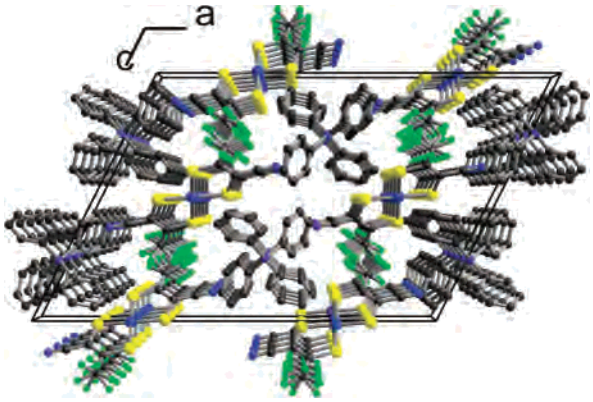

Figure 5. View of the salt **6b**.

magnetic interactions between radical anion species. The temperature dependence of the spin susceptibility confirms this analysis because it exhibits a Curie-type behavior in the 2−300 K temperature range.

Surprisingly, the structure of the PPh_4^+ salt **6b** is quasi-isostructural with that of the *n*-Bu_4N^+ salt **6a**, as seen from the almost identical crystallographic parameters (Table 1) and unit cell drawing (Figure 5). Consequently, the same temperature dependence of the spin susceptibility is obtained, with a Curie-type behavior in the 2−300 K temperature range.

Considering now the salts with the $Na(18c6)^+$ cation, in the dianionic complex **5c**, the dithiolene complex is located on an inversion center, while the Na^+ cation, in a general position in the unit cell, is included into the 18c6 cavity, with one Na−O distance slightly longer than the five others, illustrating the well-known mismatch between 18c6 and Na^+, which is too small for the 18c6 cavity. Its coordination sphere is completed by a MeOH molecule on one side and the nitrogen atom of the nitrile group of $[Ni(tfadt)_2]^{2-}$ on the other side, affording an "axle with wheels" model, where the MeOH molecules act as axle caps (Figure 6).

This specific motif has already been observed in the $Na(18c6)^+$ salt of the dianionic $Ni(mnt)_2^{2-}$, $[Na(18c6)]_2[Ni(mnt)_2][18c6]\cdot 2H_2O$,[15] with the water molecules included playing the role of the MeOH molecules to complete the coordination sphere of the sodium cation. The N···Na distance, 2.481(3) Å, compares with that reported in $[Na(18c6)]_2[Ni(mnt)_2][18c6]\cdot 2H_2O$ (2.504 Å), while the Na−

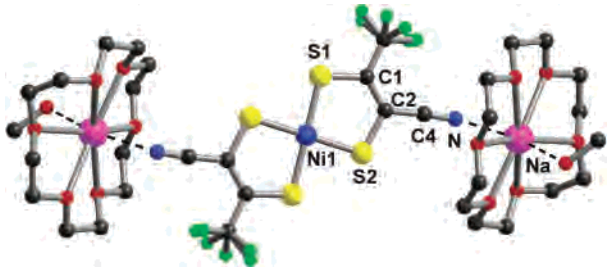

Figure 6. View of the complex **5c**·2MeOH. Important distances and angles: Na−N = 2.481(3), Na−O = 2.914(2) Å, Na−N−C4 = 145.9(2)°.

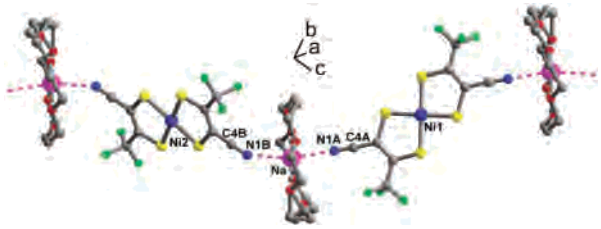

Figure 7. Heterobimetallic chain motif identified in **6c**.

N≡C(4) angle [145.9(2)°] deviates more strongly from linearity when compared with the Ni(mnt)$_2^{2-}$ salt [165.5(2)°]. These two examples also confirm the ability of the Na(18c6) motif to coordinate on both sides of the sodium cation and demonstrate the ability of nitriles to coordinate the Na(18c6)$^+$ moiety because most described examples involve exclusively the coordination of oxygen-containing molecules such as water, alcohols, or ethers.

Indeed, as shown in Figure 7, in the salt of the monoanionic, paramagnetic Ni(tfadt)$_2^{\bullet-}$ complex with Na(18c6)$^+$, two crystallographically independent Ni(tfadt)$_2^{\bullet-}$ complexes, each of them located on an inversion center, alternate with the Na(18c6)$^+$ cation to form chains running along the [111] direction of the monoclinic unit cell. The Na−N bond distances, Na−N1A = 2.434(5) Å and Na−N1B = 2.485(4) Å, compare with those reported above as well as with those reported in the only other Na(18c6)$^+$ complex coordinated by two nitrile groups described so far, that is, a tetrahedral copper(II) maleonitrile complex[15] formulated as [Na(18c6)]$_2$[Cu(mnt)$_2$] [18c6]·H$_2$O, where Na−N distances amount to 2.450 and 2.477 Å. The deviations from linearity observed in the salt of the dianion [Ni(tfadt)$_2$]$^{2-}$ are also found here because the C≡N···Na angles amount to 161.8(5)° for C4A−N1A−Na and 145.1(4)° for C4B−N1B−Na.

In the solid state, these heterobimetallic chains running along [111] and [$\bar{1}\bar{1}\bar{1}$] lead to the formation of Ni(tfadt)$_2^{\bullet-}$ stacks (Figure 8) running along the *a* axis, giving rise to uniform magnetic chains built from $S = {}^1/_2$ [Ni(tfadt)$_2$]$^{\bullet-}$ species. The temperature dependence of the magnetic susceptibility does not show, however, any susceptibility maximum in the 2−300 K temperature range, indicating that interactions within the chains along *a*, if any, are most probably very weak. Indeed, a fit to the Heisenberg chain model gives a J/k value ≈ −1 K, while a fit to the Curie−Weiss law gives a θ value of −0.5 K, confirming in both cases the very weak antiferromagnetic interactions. A rationale for this surprising behavior can be found in the

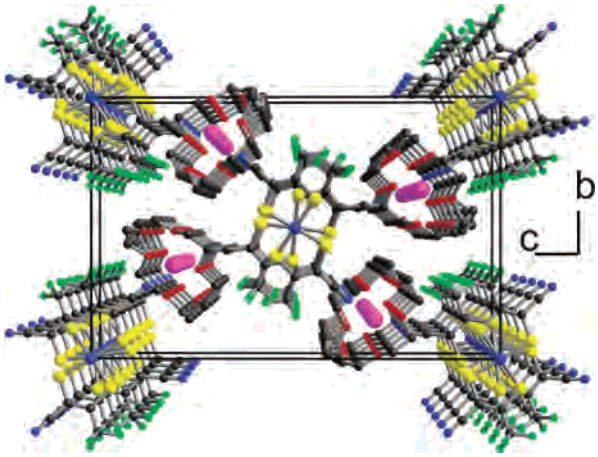

Figure 8. Perspective view of the unit cell of **6c**. Na−O bonds have been omitted for clarity.

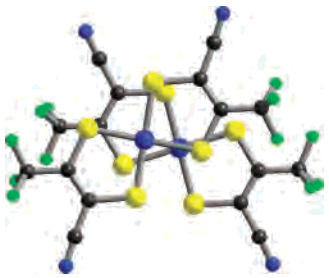

Figure 9. Detail of the overlap interaction between $S = {}^1/_2$ [Ni(tfadt)$_2$]$^{\bullet-}$ within the stacks running along *a*.

Scheme 3

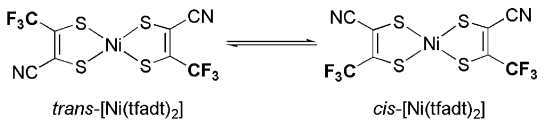

trans-[Ni(tfadt)$_2$] *cis*-[Ni(tfadt)$_2$]

precise overlap geometry within the chains. Indeed, the crystallographically independent complexes alternating along *a* are not coplanar but make a 36.58(6)° angle between mean-square planes. Furthermore, as shown in Figure 9, the overlap between neighboring molecules is most probably very weak because they organize in a criss-cross fashion with the shortest S···S intramolecular distance above 3.71 Å.

Cis−Trans Inversion Process. The tfadt ligand is one of the very few *unsymmetrically substituted* dithiolate ligands described so far, together with the adt one mentioned above. A direct consequence is the expected presence in solution of both cis and trans isomers of the square-planar complexes derived from such dithiolate ligands (Scheme 3).

While these complexes systematically crystallize in the solid state in the trans form, most probably favored by its centrosymmetric character, it can be anticipated that in solution both cis and trans isomers coexist and even interconvert. This equilibrium has been indeed observed once by ^{1}H NMR in the neutral [Ni(S$_2$C$_2$H(Ph))$_2$]^0 complex where the ^{1}H singlet resonance peak of the hydrogen atom attached to the nickel dithiolene ring observed at −60 °C splits into two peaks at −80 °C,[30] suggesting the presence of both cis

(30) Sugumori, A.; Tachiya, N.; Kajitani, M.; Akiyama, T. *Organometalics* **1996**, *15*, 5664.

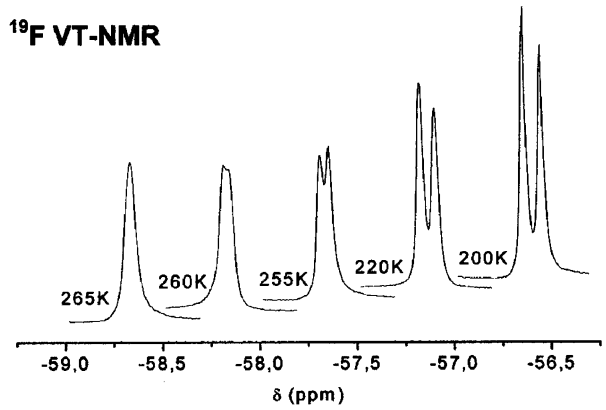

Figure 10. ^{19}F NMR spectra of **5a** at different temperatures in $CDCl_2$. The chemical shifts in the abscissa correspond to the 265 K spectrum. Other spectra have been successively shifted by 0.5 ppm.

and trans isomers, which easily interconvert at room temperature. ^{19}F VT NMR experiments were performed on the diamagnetic $[Ni(tfadt)_2]^{2-}$ complex, as n-Bu_4N^+ salt **5a**. The single resonance peak observed at room temperature for the CF_3 group at δ −58.68 splits below 260 K into two peaks with a separation that amounts to 43.18 Hz at 200 K (Figure 10).

From this behavior, we can deduce a coalescence temperature T_c of 260 K and a slow exchange rate constant k_c of 271.34 s^{-1}. Application of the Eyring equation[31] affords a first estimation of the free energy of activation at T_c, $\Delta G^{**}(T_c)$, of 51.3 kJ mol^{-1} (12.3 kcal mol^{-1}) for this interconversion process. Moreover, the separation between the two peaks ($\delta\nu$, in Hz), which increases upon cooling below the coalescence temperature, allows the simultaneous determination of the enthalpy and entropy of activation, respectively ΔH^{**} and ΔS^{**}, using a linearized form[32] of the Eyring equation (eq 1), where $k = 2\pi\delta\nu$ is the rate exchange constant determined from the frequency difference $\delta\nu$.

$$T \ln \frac{k}{T} = T\left(\ln \frac{k_B}{h} + \frac{\Delta S^{**}}{R}\right) - \frac{\Delta H^{**}}{R} \qquad (1)$$

Linear fit of the experimental data afforded the following values: $\Delta H^{**} = -7003$ J mol^{-1} and $\Delta S^{**} = -229.4$ J K^{-1} mol^{-1}. From the general $\Delta G^{****} = \Delta H^{**} - T\Delta S^{**}$ equation, we can redetermine the free energy of activation at T_c, which amounts now to 52.6 kJ mol^{-1} and compares very favorably with the value determined above from the rate constant in the slow exchange limit (51.3 kJ mol^{-1}). These results and their analysis demonstrate unambiguously that interconversion between the cis and trans forms readily proceeds at room temperature. Because only the trans form has been observed in the solid state, energy calculations with geometry optimization (DFT, UB3LYP, and LAND2Z) have been performed on the dianionic $[Ni(tfadt)_2]^{2-}$ species, in the cis and trans forms, to evaluate the energy difference between both forms. It amounts to +0.04 kcal mol^{-1}, that is, essentially zero, demonstrating that the cis and trans forms have the same energy. Therefore, the systematic crystallization of the trans form most probably finds its origin in its centrosymmetric character. The simplest isomerization mechanism that can be considered is a concerted rotation of one dithiolate ligand through a tetrahedral intermediate, as one can infer also from the distortion from planarity observed in the X-ray crystal structure of **5a** (Figure 2). However, a single-point calculation in this tetrahedral geometry raises the energy by 26.6 kcal mol^{-1} (111 kJ mol^{-1}). This value largely exceeds the estimated activation energy for the cis−trans isomerism determined from the VT NMR experiments described above because ΔG^{**} amounts to 51−53 kJ mol^{-1}. It follows that a concerted rotation of a whole dithiolate ligand to go from a trans form to a cis form through a tetrahedral intermediate without modification of the Ni−S bond lengths might not be the actual isomerization process. Other possibilities involving a breaking of one Ni−S bond with rotation around the second Ni−S bond or a lengthening of one or two Ni−S bonds are currently being investigated by calculations.

Conclusion

The square-planar nickel complexes of this novel, unsymmetrical 1,2-dithiolate tfadt ligand combine the chemical stability of the parent $Ni(mnt)_2$ or $Ni(tfd)_2$ complexes together with a stabilization of the radical anion state when compared with the $[Ni(mnt)_2]^{2-}/[Ni(mnt)_2]^{\bullet-}$ couple. The ability of the nitrile moieties to coordinate metallic centers, demonstrated here in the presence of $(18c6)Na^+$, offers numerous opportunities for the secondary coordination, through the CN moieties, of paramagnetic metal cations to form heterobimetallic chains, an issue of current strong interest in the search for single-chain magnets. Furthermore, the geometry and spin state of the complexes can be tuned by replacing the Ni in the $[Ni(tfadt)_2]$ complex by other metal cations such as Zn^{2+}, Cu^{2+}, Co^{2+}, or Au^{3+}.

Acknowledgment. Financial support from the French Ministry of Education and Research (to O.J.), from the Région Pays de Loire, and from CNRS is gratefully acknowledged. We thank Ph. Molinié (Institut Jean Rouxel, Nantes, France) for giving us access to the SQUID magnetometer, the CINES (Centre Informatique National de l'Enseignement Supérieur, Montpellier, France) for computing time, and the CRMPO (Rennes) for the HRMS measurements.

Supporting Information Available: X-ray crystallographic data (CIF), views of the molecular arrangement of **5a** and **5b**, and geometry-optimized coordinates of $[Ni(tfadt)_2]^{2-}$ and $[Ni(tfadt)_2]^{\bullet-}$. This material is available free of charge via the Internet at http://pubs.acs.org.

IC051226B

(31) (a) Eyring, H. *J. Chem. Phys*. **1935**, *3*, 107. (b) Eyring, H. *Chem. Rev.* **1935**, *17*, 65.
(32) Lente, G.; Fabian, I.; Poe, A. J. *New J. Chem*. **2005**, *29*, 759.